

AD-778 163

GEOLOGY AND MATERIAL PROPERTY
COMPARISONS FOR THE MIDDLE GUST TEST
SITES

J. E. Windham, et al

Army Engineer Waterways Experiment Station
Vicksburg, Mississippi

March 1974

DISTRIBUTED BY:

NTIS

National Technical Information Service
U. S. DEPARTMENT OF COMMERCE
5285 Port Royal Road, Springfield Va. 22151

| | |
|---------------------------------|---|
| EXPRESSION for | |
| DTIS | White Section <input checked="" type="checkbox"/> |
| DD | Self Section <input type="checkbox"/> |
| MANAGEMENT | <input type="checkbox"/> |
| JUSTIFICATION | |
| BY..... | |
| DISTRIBUTION/AVAILABILITY CODES | |
| ORL | ALL INFORMATION CONTAINED HEREIN IS UNCLASSIFIED |
| A | |

Destroy this report when no longer needed. Do not return it to the originator.

The findings in this report are not to be construed as an official Department of the Army position unless so designated by other authorized documents.

20. ABSTRACT (continued)

subsurface materials at each site are briefly described and compared herein. Details of the laboratory testing programs are reviewed, and an overview of the variations with depth of the dynamic compression and shear behavior of the materials at each site is presented. The influence of loading rate on laboratory test results is shown to be significant. Establishment of an idealized computational profile consisting of uniform zones or layers for each site is described. Through selected comparisons of available test data, some of the considerations involved in developing compatible sets of constitutive properties "representative" of the dynamic characteristics of the in situ materials occupying each of the computational profile zones are demonstrated.

PREFACE

This paper, presented by Messrs. J. E. Windham and R. A. Knott at the MIXED COMPANY/MIDDLE GUST Project Review Meeting hosted by the DoD Nuclear Information and Analysis Center, DASIAC, on 13-15 March 1973 in Santa Barbara, California, gives an overview of the MIDDLE GUST material property investigations conducted by the U. S. Army Engineer Waterways Experiment Station (WES) for the Air Force Weapons Laboratory.

The paper was prepared under DNA NWED Subtask SB209, Work Unit 11, "Laboratory Studies of the Response of Soil and Rock to Blast-Type Loadings," by personnel of the Soil Dynamics Division (SDD), WES, under the general direction of Mr. J. P. Sale, Chief, Soils and Pavements Laboratory, and Dr. J. G. Jackson, Jr., Chief, SDD.

Directors of the WES during the conduct of the study and preparation and publication of this paper were EG E. D. Peixotto, CE, and COL G. H. Hilt, CE. Technical Director was Mr. F. R. Brown.

TABLE OF CONTENTS

| | <u>Page</u> |
|--|-------------|
| PREFACE ----- | 1 |
| CONVERSION FACTORS, BRITISH TO METRIC UNITS OF MEASUREMENT ----- | 3 |
| INTRODUCTION ----- | 4 |
| GEOLOGY ----- | 5 |
| MATERIAL PROPERTIES ----- | 8 |
| Profile Composition ----- | 9 |
| Uniaxial Strain Relations ----- | 10 |
| Shear Test Results ----- | 14 |
| UX Stress Paths ----- | 16 |
| EPILOG ----- | 17 |
| FIGURES 1-17 ----- | 18-34 |
| REFERENCES ----- | 35 |

CONVERSION FACTORS, BRITISH TO METRIC UNITS OF MEASUREMENT

British units of measurement used in this report can be converted to metric units as follows:

| Multiply | By | To Obtain |
|--------------------------------|------------|-----------------------------------|
| inches | 2.54 | centimeters |
| feet | 0.3048 | meters |
| miles (U. S. statute) | 1.609344 | kilometers |
| cubic feet | 0.0283168 | cubic meters |
| pounds | 0.45359237 | kilograms |
| pounds (force) per square inch | 0.6894757 | newtons per square centimeter |
| kips (force) per square inch | 0.6894757 | kilonewtons per square centimeter |
| pounds (mass) per cubic foot | 16.0185 | kilograms per cubic meter |

GEOLOGY AND MATERIAL PROPERTY COMPARISONS
FOR THE MIDDLE GUST TEST SITES

INTRODUCTION

The U. S. Army Engineer Waterways Experiment Station (WES) was requested by the Air Force Weapons Laboratory (AFWL) to perform site investigations to support preshot ground motion calculations of the five primary MIDDLE GUST high-explosive events. Two sites, called the wet site (the location of Events I, II, and III) and the dry site (the location of Events IV and V), were explored for this purpose. Two-dimensional ground motion calculations were performed by Applied Theory, Inc., under contract to the AFWL and by Weidlinger Associates under Defense Nuclear Agency sponsorship.

To accomplish the objectives of the site investigations, a large number of undisturbed samples was obtained for use in conducting undrained static and dynamic laboratory material property tests; for conventional material classification, composition, and index tests; and for geologic examination. The laboratory test results, the drilling logs, the results of the geologic surveys, and the field seismic data (when available) comprised the information base necessary to develop an idealized computational profile for each site and to select representative dynamic constitutive properties for each profile zone. These profiles and properties were provided to the calculators prior to the shots (References 1, 2, and 3) in a form suitable for the construction of two-dimensional, nonlinear, inelastic constitutive models.

The purpose of this report is to present and compare geologic details and preshot material property summarizations for the two test sites. Specific results of the subsurface explorations, geologic investigations, and laboratory testing programs are currently being documented for each site in a series of technical reports.

In order to meet the rigid time schedules associated with Project

MIDDLE GUST, the analyses to determine preshot constitutive properties for the wet site had to proceed at a time when only about half of the results of the planned laboratory test program were available. A very cursory analysis of these test data was performed to develop preshot properties for Event I; these properties will not be discussed in this report. The time available for analysis of these data to develop preshot properties for Events II and III was more satisfactory. Except for the lack of field seismic data and some high-pressure laboratory test results, the preshot analyses for Events IV and V benefited from the availability of a full information base. As of this writing, all laboratory testing had been completed and a postshot combined-site analysis, incorporating the low-pressure data generated at Lawrence Livermore Laboratory (Reference 4), had been performed. The results of this postshot analysis are presented and compared herein, where pertinent, with the preshot properties.

GEOLOGY

The MIDDLE GUST test sites are located in Crowley County in southeastern Colorado near the small towns of Crowley and Ordway, as shown in Figure 1. Events I, II, and III were located on the west side of Bob Creek near the Colorado Canal at the wet site. The canal is the source of a shallow, perched water table in the alluvial soil overburden at this site; hence, it is called the wet site. Events IV and V were located on the west side of Nero Hill at the dry site, approximately 5 miles* northeast of the wet site; no flowing water was found within the depth explored at this site. The surface elevation in the wet site area is approximately 4,400 feet above mean sea level (msl); the dry site surface elevation is approximately 4,600 feet msl.

According to the geologic literature, the sites lie within the relatively flat to gently rolling Great Plains physiographic province. The locations of the sites relative to their geologic stratigraphic

* A table of factors for converting British units of measurement to metric units is presented on page 3.

columns are shown in Figure 2. Both sites are situated in the Cretaceous Pierre Formation, which is primarily composed of clay shales generally deposited in a shallow marine environment approximately 65 million years ago. In the site region, the Pierre is underlain by an estimated 6,800 feet of nearly horizontal Mesozoic and Paleozoic sedimentary rocks overlying Precambrian crystalline basement rocks. It is estimated that a maximum of 4,000 feet of Cenozoic and Mesozoic sediments has been removed from the general area by periodic post-Cretaceous erosion, leaving the currently exposed surfaces of the Pierre Formation. In recent geologic times, a 9-foot-thick alluvial deposit of mixed sands, silts, and clays has accumulated over the Pierre clay shale at the wet site. No major geologic structural features (faulting, folding, etc.) are believed to exist in the immediate vicinity of either site.

At the wet site, the deepest sample boring penetrated to a depth of 500 feet, where it is believed to have encountered the transition materials comprising the Pierre/Niobrara interface. The deepest dry site sample boring penetrated to a depth of 250 feet. The Pierre/Niobrara interface was not encountered at the dry site; it is estimated to be at a depth of approximately 750 feet. The shale at the dry site is approximately 250 feet higher in the depositional sequence, i.e., it is geologically younger, than the wet site shale (Figure 3). This is due to variations in surface topography in the general area as well as to a slight dip in the shale bedding of approximately 15 feet per mile toward the north, as illustrated in Figure 3. As a result, the clay shales encountered at the two sites were not identical. The siltstone marker bed shown in Figure 3 was used as a cross-correlation index between the two sites. This marker bed was consistently encountered at a depth of approximately 130 feet in the borings at the wet site and is believed to have been identified by electric logging techniques at the dry site, where the electric log borings were augered to a depth of 420 feet, 170 feet deeper than the deepest sample boring.

The wet site is composed of an alluvial soil overburden approximately 9 feet thick overlying approximately 14 feet of weathered, fractured clay shale; this in turn overlies a more competent clay shale

bedrock as shown in Figure 4. Two regional joint sets were found in the shale (Reference 5). One set, spaced at intervals of 6 to 8 feet, has a strike that varies between $N56^{\circ}E$ and $N62^{\circ}E$, with a dip of $85^{\circ}NW$; the second set, spaced at intervals of 10 to 14 feet, has a strike that varies between $N20^{\circ}W$ and $N30^{\circ}W$, with a dip of $86^{\circ}NE$. The ground surface at the site is relatively flat, and the depths to important interfaces are essentially constant. The soil overburden is subdivided by a groundwater table, the depth of which depends upon the water level in the surrounding Colorado Canal. At the time that samples were taken from the site, the groundwater table was at a depth of approximately 4 feet. The presence of this groundwater has resulted in significant differences in material properties between the overburden soils above and below the water table; in addition, it has influenced weathering processes in the fractured clay shale below the overburden, e.g., it has partially "healed" some previous fractures.

The dry site comprises an average of 28 feet of weathered, fractured clay shale overlying a more competent, relatively impervious clay shale, as shown in Figure 4. Using thermal-infrared image techniques, the U. S. Geological Survey identified three sets of joints in the weathered shale, striking at about $N50^{\circ}E$, $N45^{\circ}W$, and $N20^{\circ}-25^{\circ}W$, in order of prominence (Reference 6). Strikes roughly corresponding to these, with nearly vertical dips, were also observed in pits excavated at the site. The ground surface of the site generally dips from east to west on a slope of about 1:50. The depth of the weathered shale/competent shale interface varies in an east-west direction across the site from approximately 23 feet at the eastern site boundary to about 32 feet at the western boundary. The depth of weathering is primarily a function of climatic conditions and subsurface drainage. The degree of weathering generally decreases and the material competency gradually increases with increasing depth toward the weathered shale/competent shale interface; however, there is an approximately 8-foot-thick weathered unit just above the competent shale that does not follow this general trend. The shale in this unit contains considerably more gypsum than the materials above as the result of greater water accumulation

during times of precipitation. Consequently, this unit has a lower density, a higher porosity, and a lower degree of saturation than the adjacent units.

Additional distinctions exist between the clay shales at the two sites. As indicated in Figure 5, a large number of pyritic nodules and carbonate concretions were encountered in the upper 150 feet of clay shale at the wet site; no pyritic nodules were found at the dry site. These nodules primarily served to complicate sampling and testing of the wet site materials. Below a depth of 150 feet at the wet site, the pyritic nodules essentially disappeared, but the degree of calcareous cementation increased. The clay shale below 340 feet at the wet site was found to be very hard and highly calcareous. At corresponding depths, the wet site clay shales were more calcareous than the dry site clay shales.

In the Event III ground zero (GZ) boring at the wet site, a change in the dip of the beds was encountered below a depth of 130 feet. The dip increased gradually to about 8 degrees at a depth of 200 feet, then changed continuously to about 25 degrees at a depth of 250 feet. Thereafter, it remained at about 25 degrees (to 500 feet). In the 250-foot-deep Event II GZ boring located 800 feet to the west, no change in the dip of the beds was observed. Whether the dipping beds in the Event III boring represent previous faulting or uplifting or merely resulted from bending of the drill stem is not known. Other than the very slight 15 foot/mile dip described previously, no dipping beds were encountered at the dry site throughout the depth sampled (250 feet).

MATERIAL PROPERTIES

The WES laboratory testing programs for the wet and dry sites generally consisted of the following tests:

1. Routine classification and index tests to identify the soil and clay shale constituents.
2. Conventional water content and density determinations to establish the in situ composition properties.
3. Static and dynamic uniaxial strain (UX) tests up to 10,000-psi vertical stress to develop stress-strain relations.

4. Static null UX tests with radial stress measurements to assist in establishing stress paths for a state of uniaxial strain.
5. Static and dynamic triaxial compression (TX) tests at confining pressures up to 10,000 psi to assist in establishing failure envelopes and to provide appropriate moduli data for developing and cross-correlating representative constitutive properties.

In addition, some static direct shear tests were performed on wet site clay shale samples in directions parallel and perpendicular to the bedding planes, and a number of indirect (Brazil) tension tests were performed to investigate shear and tensile strength anisotropy.

The data obtained from the laboratory testing programs and the geologic investigations, along with the field seismic data (when available) and the boring logs, were analyzed to develop an idealized computational profile for each site and to establish dynamic constitutive properties most representative of the live loading characteristics of the in situ material in each profile zone. A typical set of these constitutive properties is shown in Figure 6. The set includes representative UX stress-strain relations, the slopes of which define the constrained modulus M ; a representative failure envelope; and representative paths of principal stress difference versus mean normal stress for uniaxial strain. The slopes of the UX stress paths supply information about other material coefficients; for example, the familiar shear modulus G , bulk modulus K , and Poisson's ratio ν of Hookean elastic theory. This set of representative properties provides the code calculator with a complete stress tensor-strain tensor relationship to which he can fit his mathematical constitutive model.

Profile Composition

The preshot idealized geologic and computational profiles established for the MIDDLE GUST wet and dry sites are compared in Figure 7. The water contents and dry and wet unit weights selected as representative of the in situ materials in each zone are compared in Figure 8; the corresponding idealized air void contents are shown in Figure 9. The air void contents are significantly lower at the wet site than at the dry site; this is a function of material type as well as the presence

of the groundwater at the wet site. Zone 6 of the dry site stands out in Figures 8 and 9; this is the highly gypsiferous unit previously discussed.

For preshot computational purposes, the MIDDLE GUST wet site was idealized to a depth of 500 feet (the maximum depth sampled) by ten zones, the zone thicknesses generally increasing with depth. To establish a rational model of the sandy clay overburden, three relatively thin zones (two above the water table and one below) were recommended. This fine zoning was required to account for the large decrease in air voids (and, therefore, compressibility) occurring through the overburden (Figure 9). The fourth and fifth zones (comprising, respectively, a relatively soft, highly weathered clay shale and a moderately hard, but still extensively fractured, weathered clay shale) were sufficiently different from each other and the adjacent materials to warrant separate treatment. Zones 6 through 9 were chosen to model the hard, unweathered clay shales that increase in density, calcareousness, and general competency with depth. Zone 10 models the very hard, highly calcareous clay shale representing the probable Pierre/Niobrara transition.

The MIDDLE GUST dry site was idealized to a depth of 250 feet (the maximum depth sampled) by eleven computational zones. Zones 1 through 5 define the weathered, fractured clay shales in which the degrees of weathering and fracturing decrease with depth. The material in Zone 6, the anomalous gypsum-rich zone, is more weathered than the material in Zone 5. As at the wet site, the relatively unweathered, competent clay shales at the dry site (Zones 7 through 11) become harder and more competent with depth.

Uniaxial Strain Relations

In order to demonstrate some of the considerations involved in data analyses, comparisons of dynamic UX test data with recommended preshot stress-strain relations for selected zones are presented in this section. In addition, the loading UX stress-strain relations recommended preshot for each zone are compared for each idealized site profile. Finally, the initial constrained moduli M_1 associated with the recommended UX relations are compared with the field seismic constrained moduli for each site.

Figure 10a compares the dynamic UX stress-strain data available preshot for Zone 4 (weathered clay shale) of the idealized wet site profile with the recommended relation. Figure 10b shows a similar comparison for the unweathered clay shale of wet site Zone 7. The composition properties for each zone are also shown in Figure 10. These properties include the water content W in percent by weight of soil solids; the dry unit weight γ_d in pounds of solids per cubic foot of soil; the wet unit weight γ in pounds of water and solids per cubic foot of soil; the specific gravity of soil solids G_s ; the degree of saturation S in percent of total void volume filled with water; and the volumes of air V_a , water V_w , and solids V_s as fractions of the total volume.

The material in Zone 4 is a soft, variably weathered clay shale; however, its constitutive properties are more like those of a very competent soil rather than those of a good, sound shale. From top to bottom of this zone, there is a decrease in the volume of air-filled voids. This composition property controls the strain level at which "lock-up," or fully saturated behavior, occurs. The individual test results in Figure 10a typify the variation of air voids through the zone. The recommended relation was based on the actual data but was keyed to the most representative air void content in the zone.

The quality of the samples cored from the deeper, more competent clay shales at both sites varied greatly. Sampling these materials was difficult in that under the stresses induced by coring, the materials fractured easily along the bedding planes, indicating that they possessed little tensile strength normal to these planes.* When, as is the usual WES procedure, a cored sample is intended for uniaxial strain testing purposes, it is retained in its 5-1/4-inch-OD by 5-inch-ID steel Shelby tube to minimize disturbance due to in situ stress/strain relief. It is not until after the test specimen has been prepared (Reference 7) and the test conducted that the internal quality of the specimen can be

*Brazil tests conducted on the unweathered clay shales indicated that tensile strength parallel to the beds was approximately an order of magnitude greater than tensile strength normal to the beds.

thoroughly observed. Hence, many UX tests were conducted on disturbed samples. Although X-radiography techniques aided in selecting the better quality specimens for UX testing, the method was not always successful with these large-diameter cores; however, the method was extremely valuable for selecting good quality NX-size cores for TX testing purposes.

The data shown in Figure 10b typify the types of test results generated with the samples obtained from the more competent clay shale zones at both sites. Specimens A and B were of very good quality; they contained no observable man-made horizontal fractures and they were fully constrained laterally, i.e., they fit tightly against their Shelby-tube rings. Specimens C and D were only partially constrained and contained minor drilling-induced horizontal fractures. Specimen E made erratic lateral contact with its Shelby-tube ring, and Specimen F contained major mud-filled horizontal fractures. Obviously, Specimens C, D, E, and F were not representative of the intact material, nor could they have truly deformed in uniaxial strain. Hence, only Specimens A and B were qualified to comprise the data base for developing the preshot relation for this zone.

All of the UX loading stress-strain relations recommended preshot for each site are compared over the 0- to 2,000-psi stress range in Figure 11. Samples from wet site Zones 1 and 3, representing the overburden soils, were initially quite compressible; however, once the air voids were closed and the air was dissolved in the water, these materials became highly incompressible, behaving like mixtures of solid particles and water. Samples from Zones 4 and 5, the nearly saturated, fractured clay shale zones, were initially stiffer than those from the overlying soils, but their ultimate compressibilities were also strongly controlled by the water.* At the 2,000-psi stress level, the dry site weathered shales were more compressible than the wet site

*If the perched groundwater had not been present at the wet site, the air voids as well as the compressibility characteristics of the Zones 4 and 5 clay shales would have been more like those of the dry site weathered clay shales (Zones 1 through 6).

weathered shales due to the differences in air void contents (Figure 9). The stiffnesses of the unweathered shales at both sites were generally comparable. Except for the anomalous material in Zone 6 at the dry site, the general trend for samples from both sites was for compressibility to decrease with increasing depth.

The initial slopes of the curves shown in Figure 11 are presented as a function of depth for each site in Figure 12 (dashed lines), where they can be compared with the constrained moduli calculated from the field seismic velocity data (solid lines). The dotted lines in Figure 12 indicate recent modifications to the preshot properties resulting from the WES postshot combined-site analysis (which primarily benefited the wet site). There is considerable scatter in the field refraction seismic data obtained from the dry site, particularly in the weathered materials (Zones 1 through 6); the question marks on the solid lines in this region (Figure 12b) indicate that the interpretation of these seismic data is tentative. In the deeper, more competent shales, the seismic moduli plotted are those obtained by Birdwell borehole logging techniques.

Figure 12 indicates that the seismic moduli in the competent shales at both sites (below Zone 5 at the wet site and below Zone 6 at the dry site) are quite similar. It also shows that the seismic moduli are considerably greater than the recommended initial moduli at both sites. Although wet site field seismic data were available prior to the execution of Events II and III, seismic moduli were not appended to the properties recommended for preshot calculations nor were the code constitutive models modified to accept such appendages. At the time the code models were being fitted to the preshot properties, the seismic moduli, had they been included, would most likely have been arbitrarily modeled up to stress levels of only a few pounds per square inch, thus precluding any noticeable effects in code output except at the very far out ranges (e.g., beyond the 50-psi contour). Field seismic data were not available for the dry site until after Events IV and V had been executed.

Shear Test Results

The results of triaxial compression tests conducted at various loading rates are compared in Figure 13 with the recommended preshot failure envelopes for wet site Zone 4 and dry site Zone 8; these zones were selected to typify the strength characteristics of the soft, weathered clay shale and the hard, unweathered clay shale. Both materials exhibited significant strength increases under dynamic conditions. Also, the unweathered clay shale was an order of magnitude stronger than the weathered material.

The shear strength differences among the soils at the wet site and the weathered and unweathered clay shales at both sites are clearly illustrated in Figure 14, which compares the recommended preshot failure envelopes for each zone of each computational profile. Of all the materials at both sites, the wet site soils are the weakest; their ultimate strengths are significantly influenced by the water. The next strongest materials are the weathered shales at the wet site; they possess more strength than the soils, but are weaker in general than the weathered shales at the dry site. Although the water also influences the ultimate strengths of the weathered shales, they are inherently stronger than the soils, water or no water. There are abrupt increases in strength at the transition from the weathered to the unweathered clay shales at both sites, followed by continuous strength increases (and accompanying density and cementation increases) with increasing depth.

Only static TX data were obtained for the wet site clay shales below a depth of 15 feet.* Also, at the time of the wet site preshot analysis, no constitutive property data of any kind were available for the material below 125 feet. Hence, factors on the order of 40 percent were used to develop dynamic failure envelopes from the representative static envelopes for Zones 5, 6, and 7, and experience and judgment were called upon to assign properties to Zones 8, 9, and 10. As

*WES high-quality dynamic TX equipment did not become fully operational until the dry site investigation was under way, after which time the device was used extensively.

indicated by the data in Figure 13b, the static-to-dynamic factors for Zones 5, 6, and 7 should have been on the order of 100 to 200 percent. In addition, completion of the wet site data base showed that the estimated strengths for Zones 8, 9, and 10 were too low. Therefore, the failure envelopes shown in Figure 14a for the unweathered clay shales should be increased, some by as little as 50 percent and some (the materials below 125 feet) by as much as 200 percent.

A comparison of only the static TX data from both sites at comparable depths shows that the wet site unweathered shales are generally stronger than those of the dry site; this is in keeping with the higher density and greater cementation of the wet site materials. In addition, direct shear tests conducted on vertically and horizontally oriented clay shale specimens indicated no compressive strength anisotropy; these data also correlated well with the TX strength results, all of which had to be obtained using vertically oriented specimens.

In addition to strength information, TX tests also supply data that can be used to determine Hookean parameters such as Young's modulus E , as well as G , K , and ν (the latter three quantities only if, as was done for these investigations, the complete strain tensor is determined). Figures 15 and 16 summarize the ranges of initial loading Young's moduli E_i and initial loading shear moduli G_i , respectively, determined from all of the static and dynamic TX data obtained for both sites. The data bands do not represent scatter! Rather, they represent the effects of confining pressure; the associated confining pressures spanned the range from 0 to 10,000 psi. Hence, data points from the lowest confining pressure tests crowd the lower band edges, and data points from the highest confining pressure tests crowd the upper band edges. The purpose of presenting these data in this form was to provide a simplified comparison of the gross shear response characteristics of the various materials at each site.

Figures 15 and 16 indicate two major effects: (1) E_i and G_i of the unweathered clay shales at both sites are approximately one order of magnitude greater than E_i and G_i of the soils and weathered shales; and (2) E_i and G_i in the clay shales are moderately

rate-sensitive, the sensitivity being approximately the same as that of the shear strength (Figure 13). A third effect is that the wet site unweathered clay shales exhibit slightly greater Young's moduli and shear moduli than the corresponding dry site shales, which is logical due to the higher density and degree of cementation of the wet site materials.

UX Stress Paths

To complete the representative constitutive properties package, paths of principal stress difference versus mean normal stress for dynamic uniaxial strain were developed for each profile zone. These paths were generally based on interpretations of data obtained from special static UX null tests in which the lateral stress was measured; however, the static and dynamic modulus data obtained from the TX tests were also used in developing the dynamic UX paths.

Figure 17 compares the recommended preshot UX stress paths for wet site Zones 2 (soil) and 7 (unweathered clay shale) with their respective failure envelopes. This figure is presented to illustrate some fundamental behavioral differences in uniaxial strain between normally consolidated soils and highly overconsolidated saturated clay shales.

Because a normally consolidated soil undergoing shear exhibits little or no tendency to dilate, its loading UX stress path can reach the failure envelope defined by shear tests at quite low shear and normal stress levels (Figure 17a). For continued loading, the path generally follows the failure envelope. For subsequent unloading, the paths become flatter as the maximum pressure level increases; this implies that the unloading shear modulus is approximately constant beyond some critical pressure level or that it increases at a slower rate than the bulk modulus increases.

In shear tests on overconsolidated saturated clay shales, on the other hand, there is usually a tendency toward dilatancy accompanied by work-hardening and brittle failure phenomena. However, dilatancy cannot occur if lateral strains are suppressed. As a result, the development of shear stresses during loading in uniaxial strain is also suppressed

and the UX stress path stays well below the shear failure envelope over a large range of pressure (e.g., $0 \leq P \leq 5,000$ psi). At sufficiently high pressures, the preconsolidation history of the clay shale will be exceeded and the material will respond as though it were normally consolidated, i.e., it will exhibit ductile, nondilatant behavior, and the UX path will approach the shear failure envelope. Unloading stress paths for saturated clay shales tend to parallel the loading path (Figure 17b); this implies elastic (i.e., reversible) or nearly elastic behavior.

EPILOG

In addition to taking a closer look at the effects of sample disturbance, WES is continuing analyses of the field and laboratory data obtained from the two MIDDLE GUST site investigations with emphasis placed on evaluating factors such as anisotropy, rate effects, tensile strength and brittle-ductile failure and shear-induced volume change phenomena, almost all of which were excluded from the preshot calculation models and each of which may have contributed somewhat to the gross discrepancies between the code calculations and the field motion records.

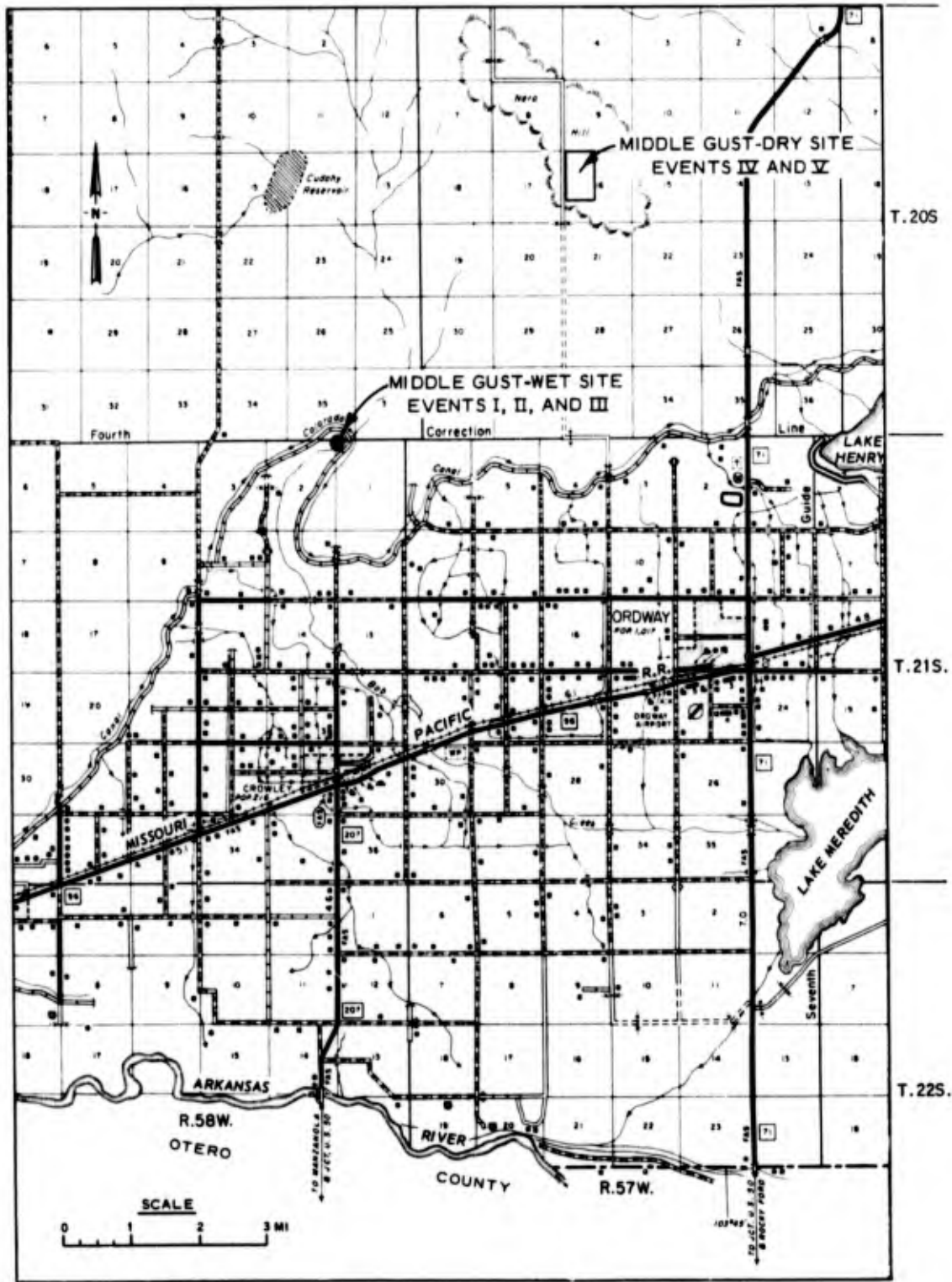


Figure 1. Site location map.

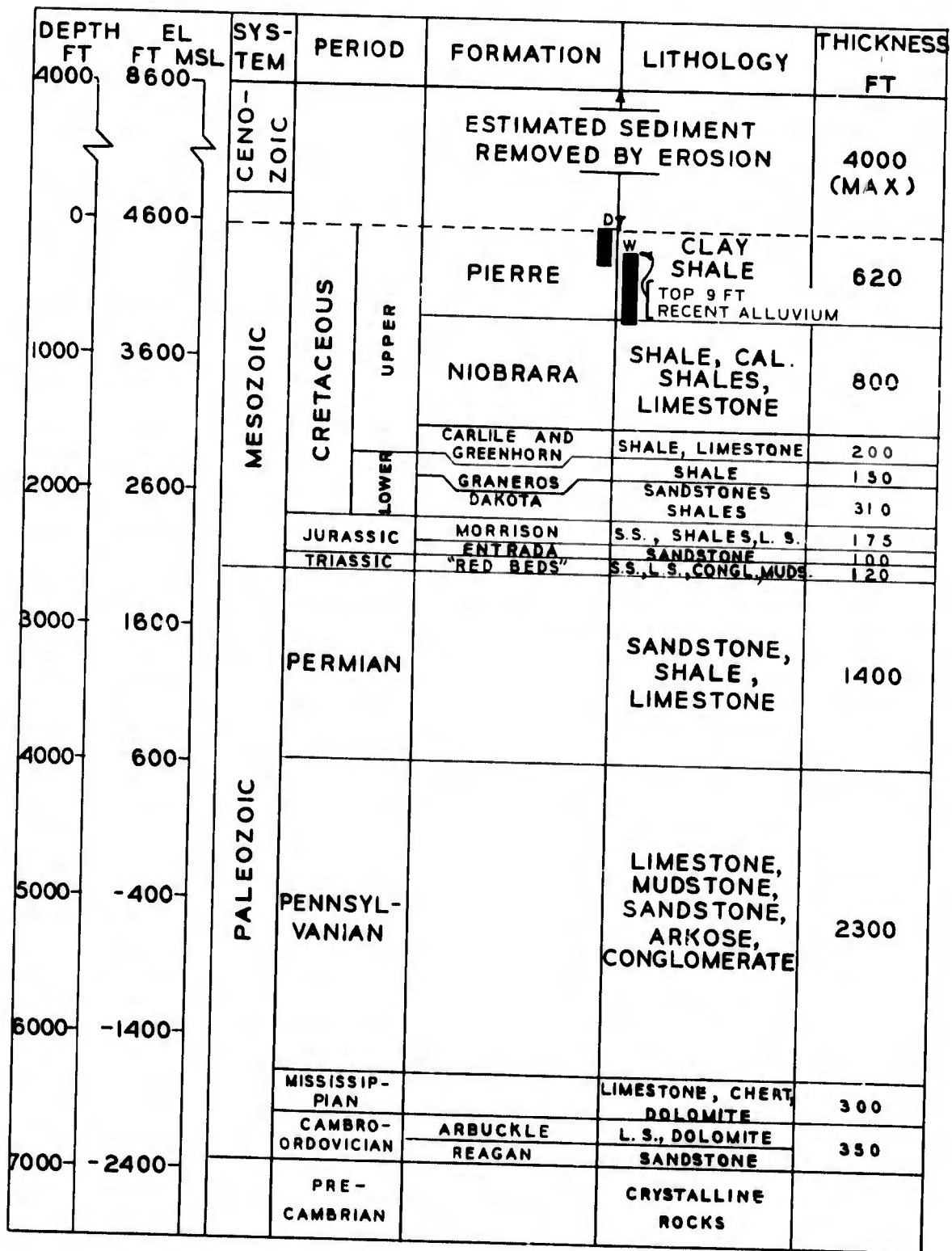


Figure 2. MIDDLE GUST geologic stratigraphy.

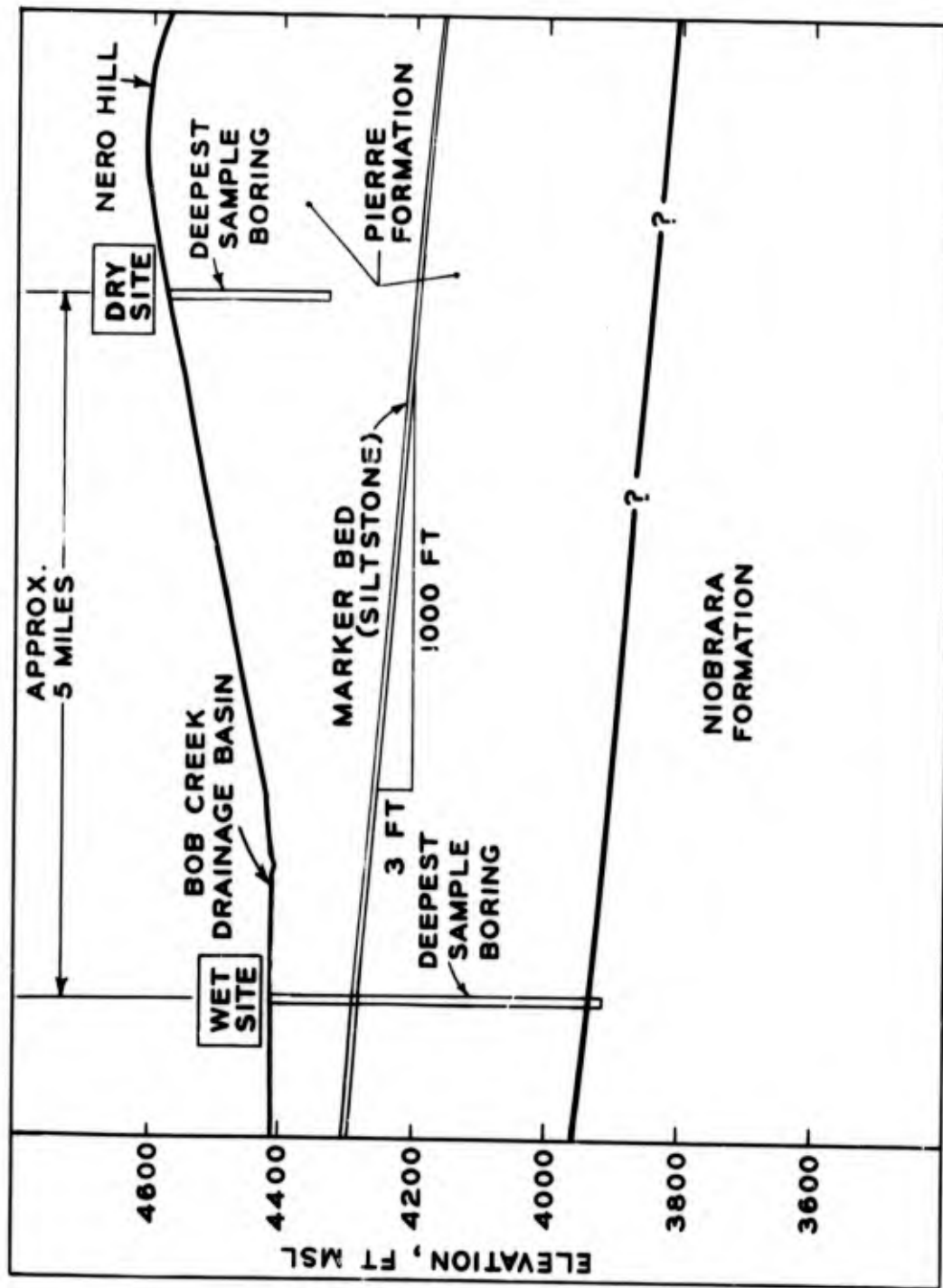
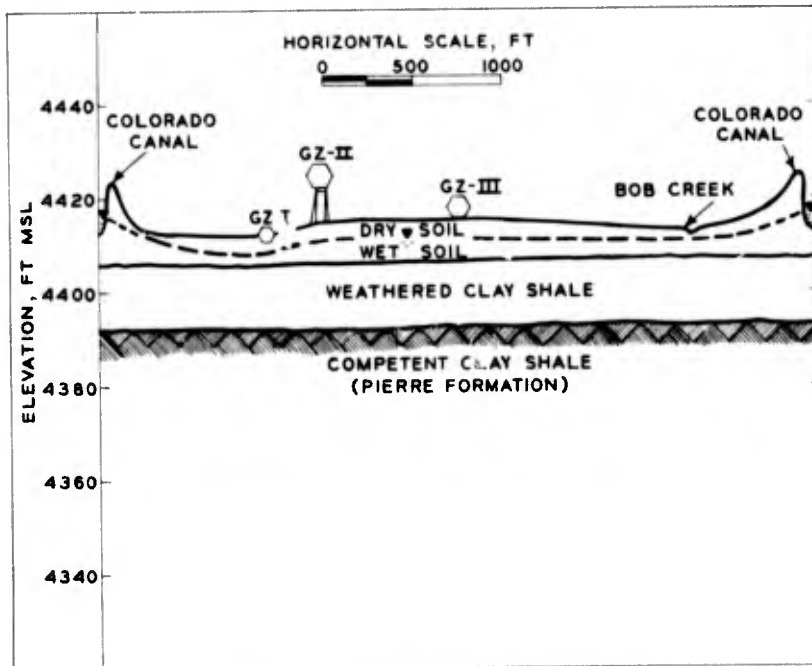
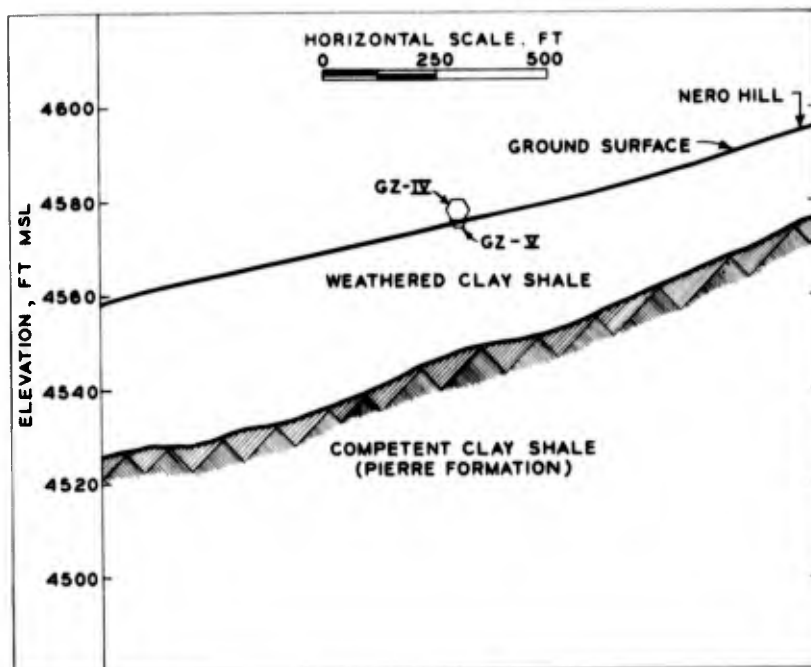


Figure 3. Generalized cross section between MIDDLE GUST wet and dry sites.



a. WET SITE - EVENTS I, II, AND III



b. DRY SITE - EVENTS IV AND V

Figure 4. MIDDLE GUST generalized near-surface profiles viewing north.

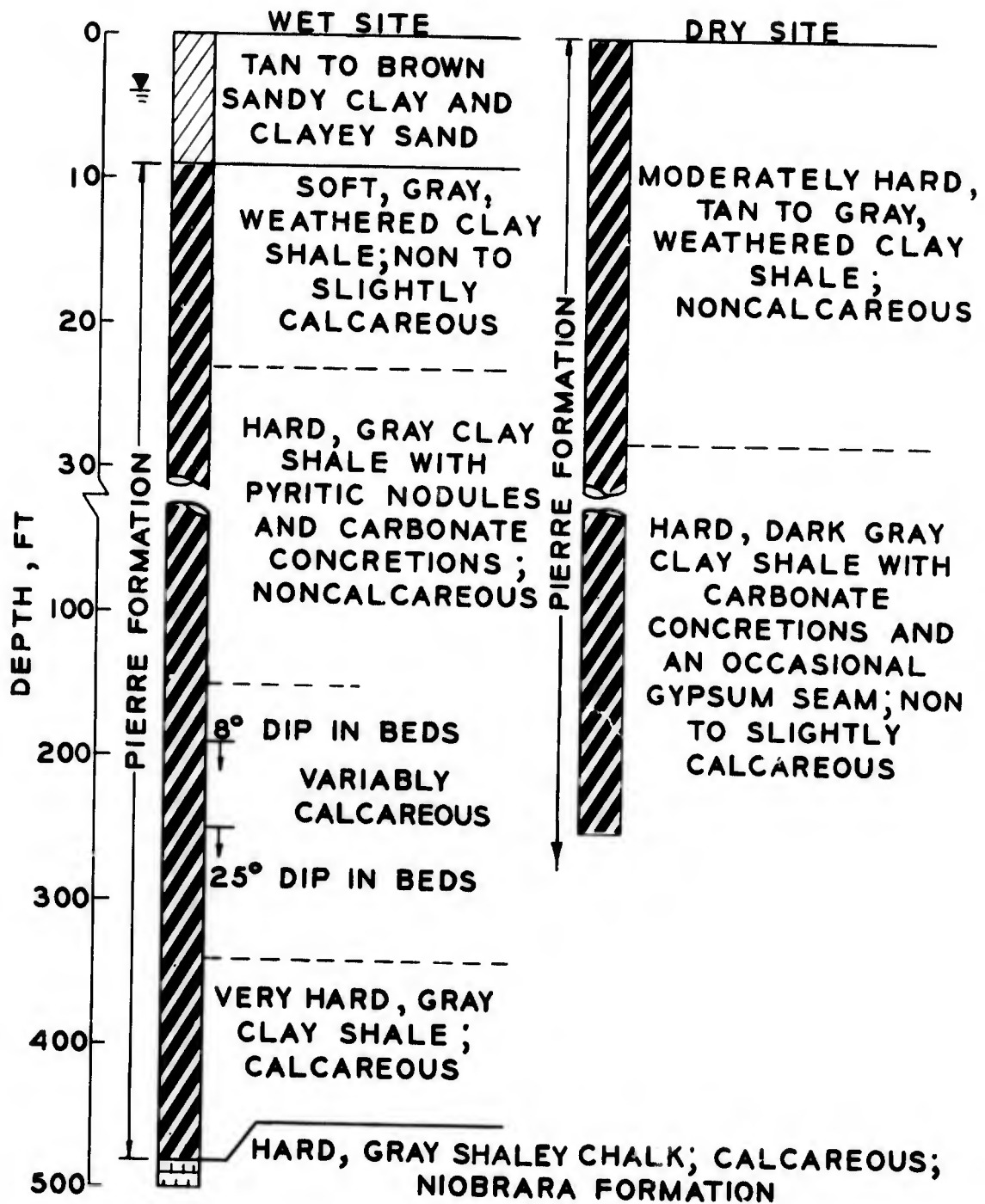
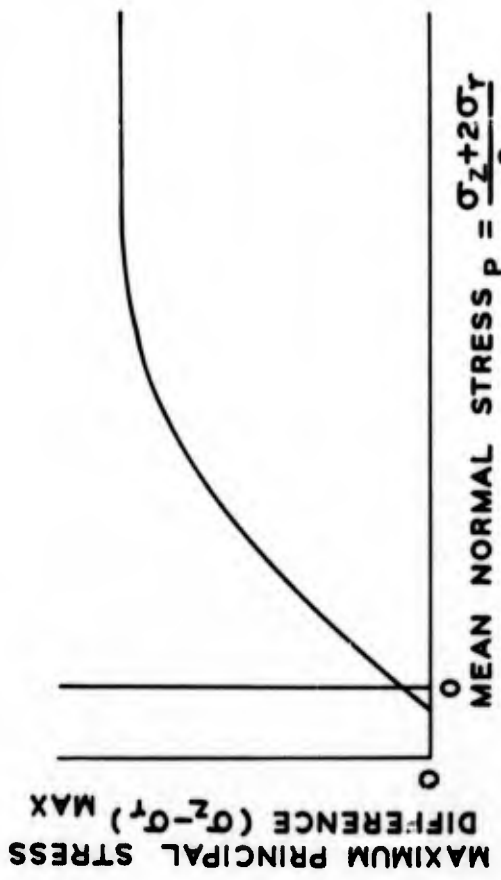
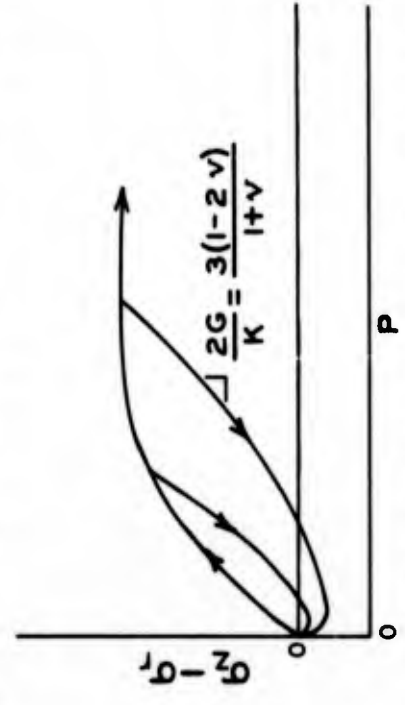


Figure 5. Descriptive geologic profiles, MIDDLE GUST wet and dry sites.



b. REPRESENTATIVE FAILURE ENVELOPE



c. REPRESENTATIVE UX STRESS PATHS

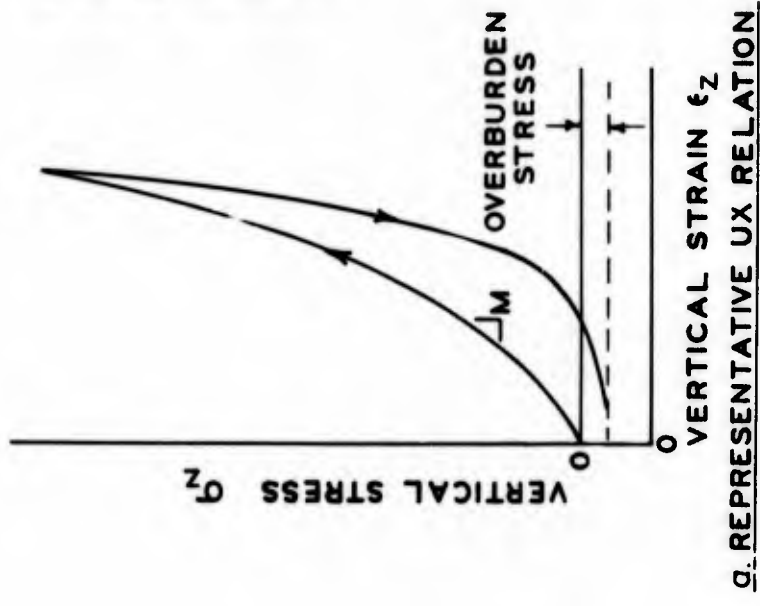


Figure 6. Typical set of constitutive properties recommended for live loading in each computational zone.

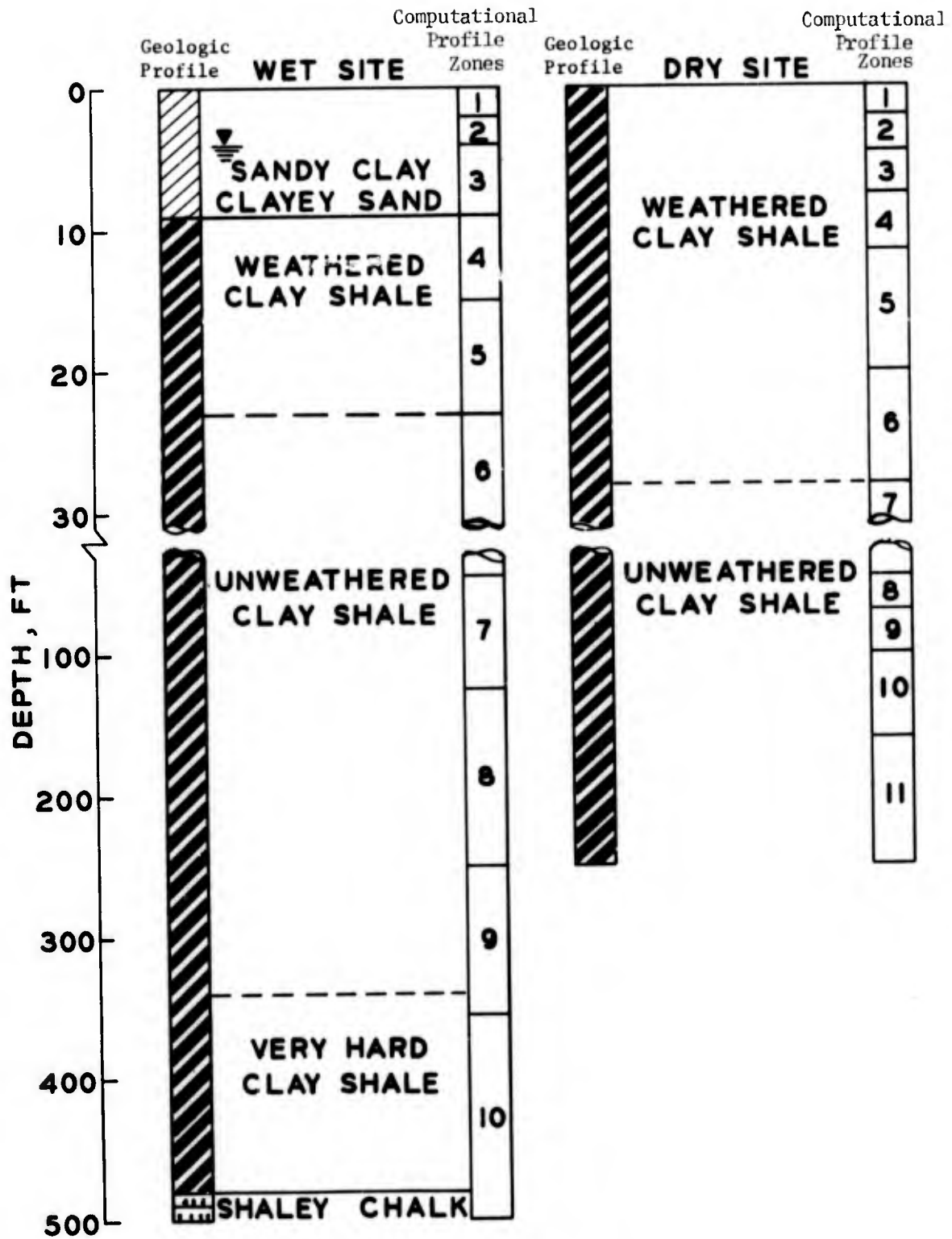
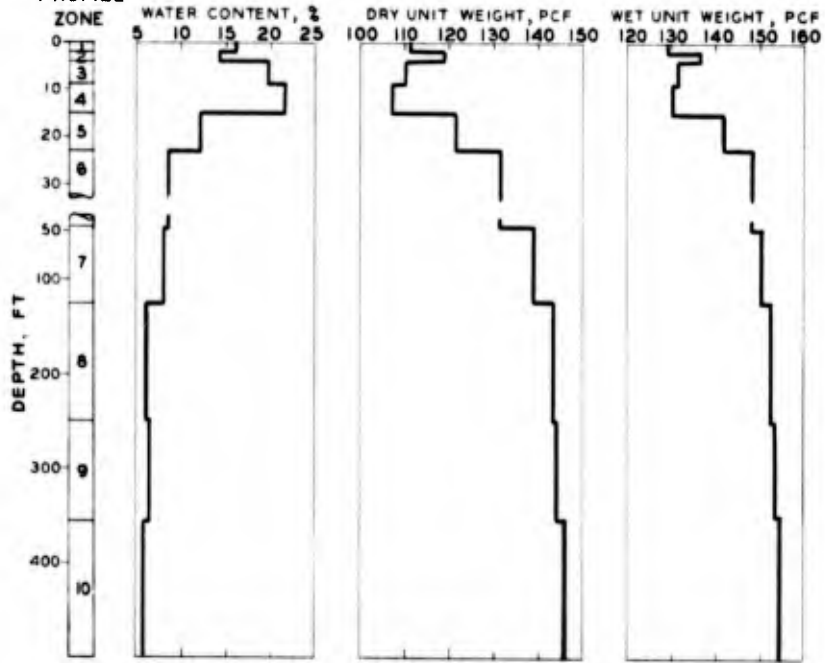


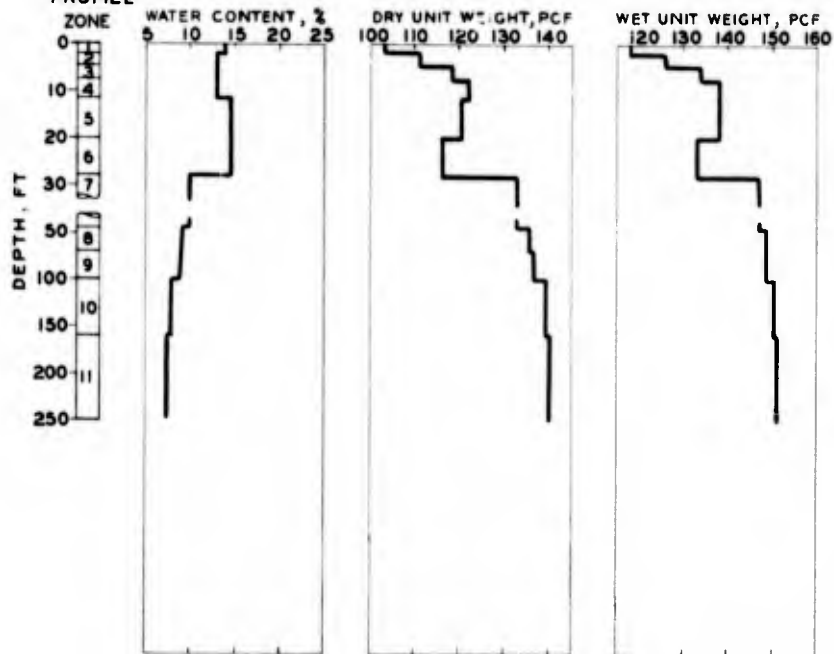
Figure 7. Idealized preshot geologic and computational profiles for MIDDLE GUST wet and dry sites.

COMPUTATIONAL
PROFILE



a. Wet site.

COMPUTATIONAL
PROFILE



b. Dry site.

Figure 8. Idealized composition properties for MIDDLE GUST preshot computational profiles.

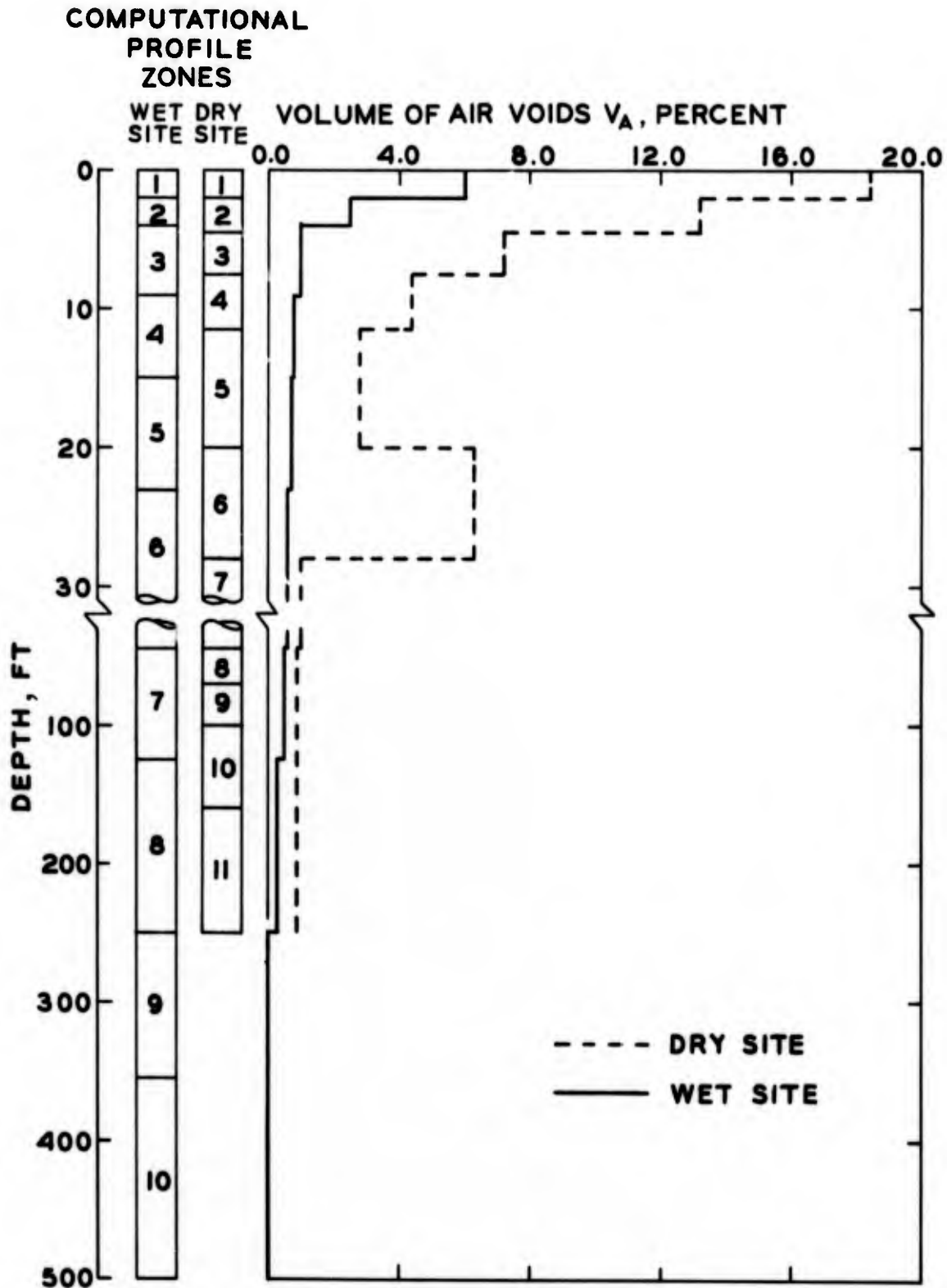


Figure 9. Idealized air void percentages for MIDDLE GUST wet and dry site preshot computational profiles.

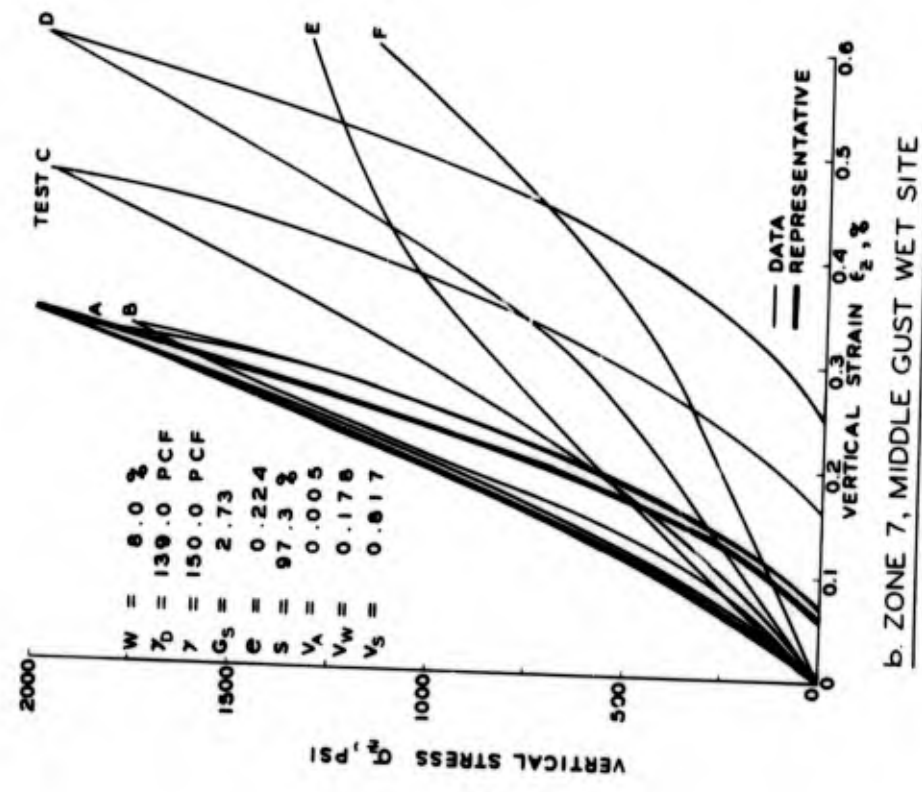
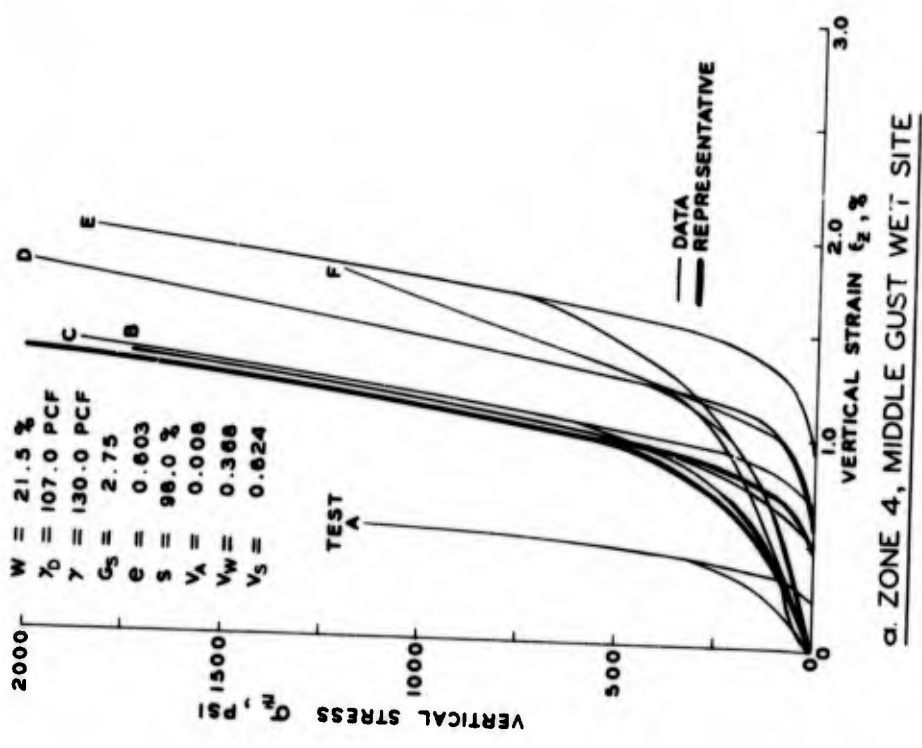
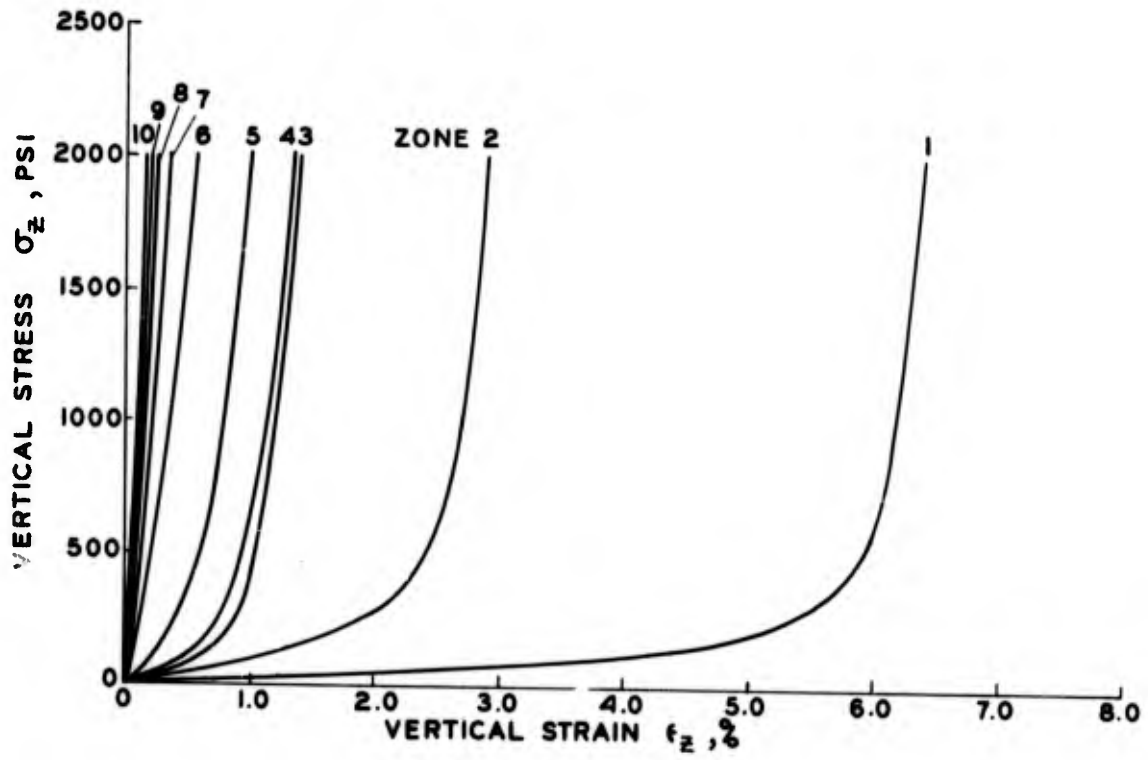
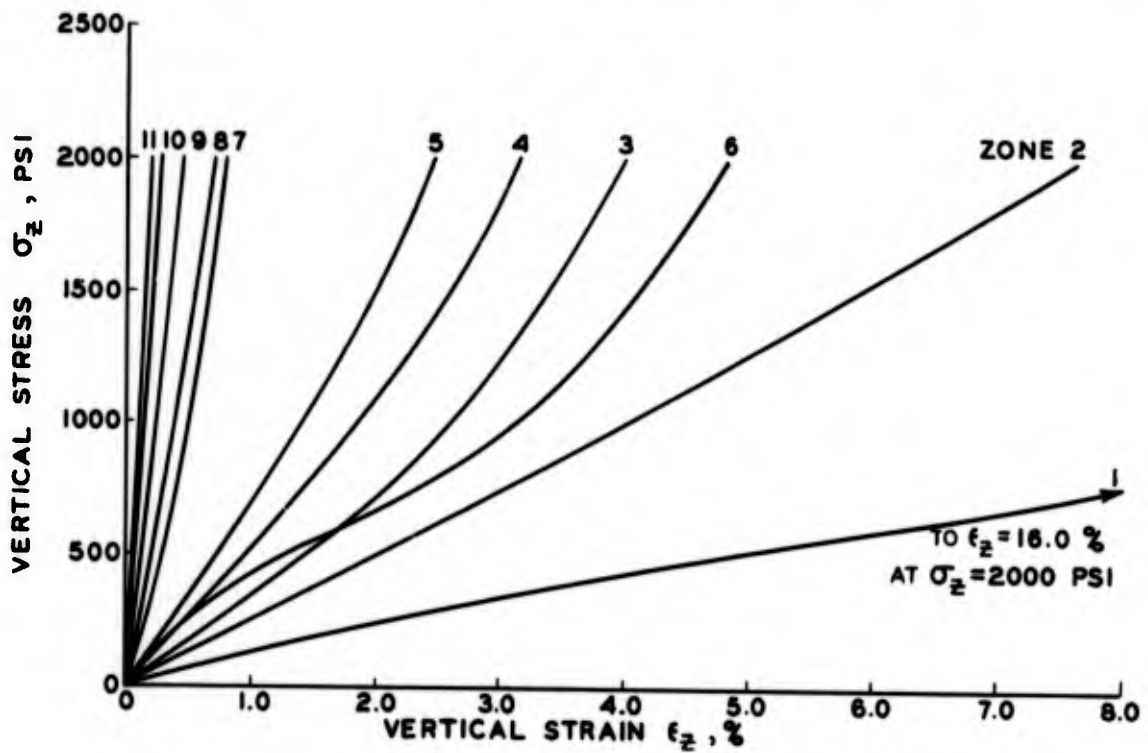


Figure 10. Representative preshot dynamic uniaxial strain relations compared with typical data sets for selected zones.

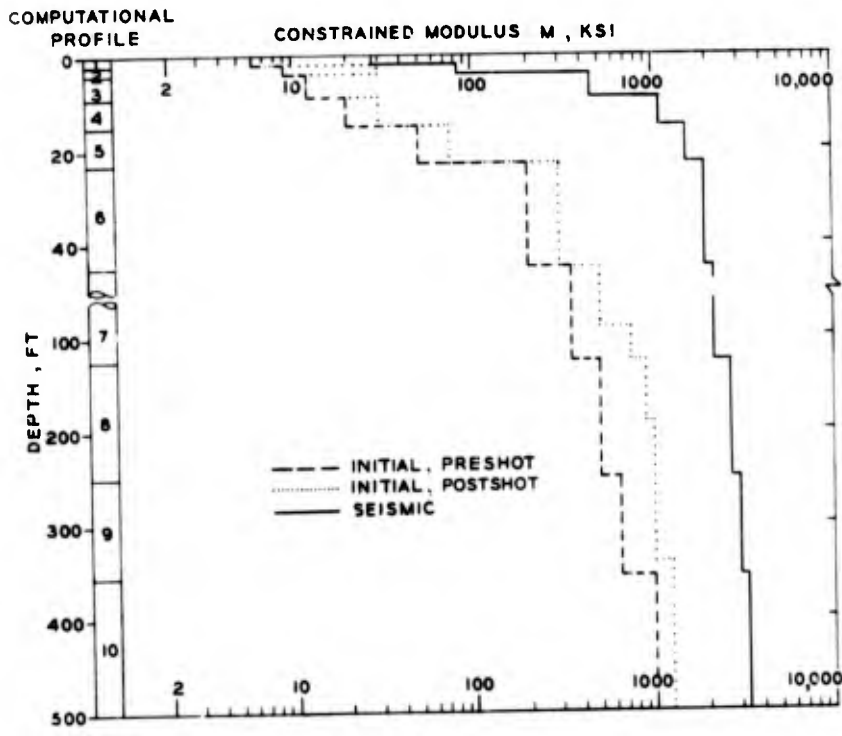


a. Wet site.

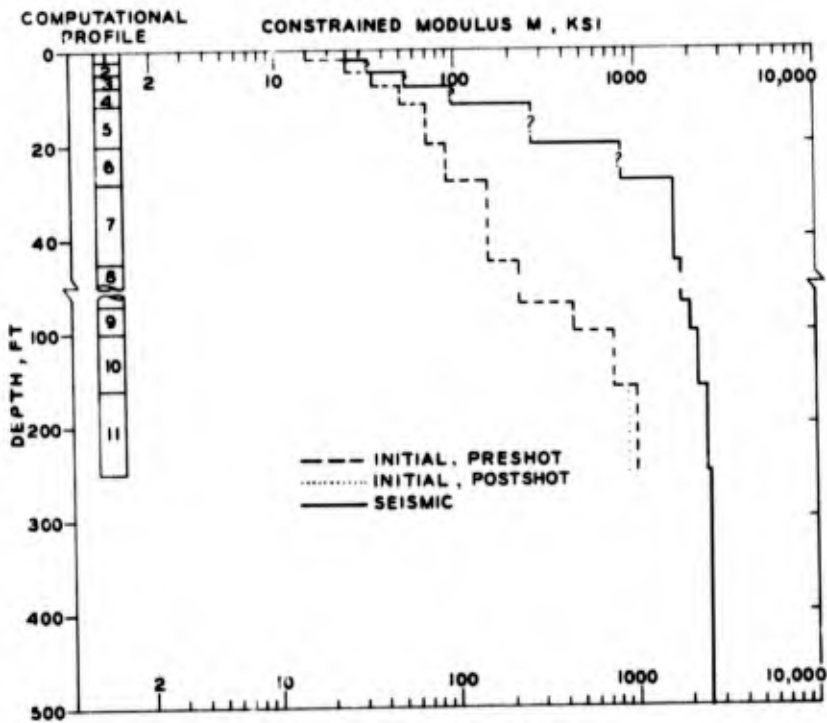


b. Dry site.

Figure 11. Comparison of dynamic uniaxial strain loading relations recommended preshot for MIDDLE GUST.



a. Wet site.

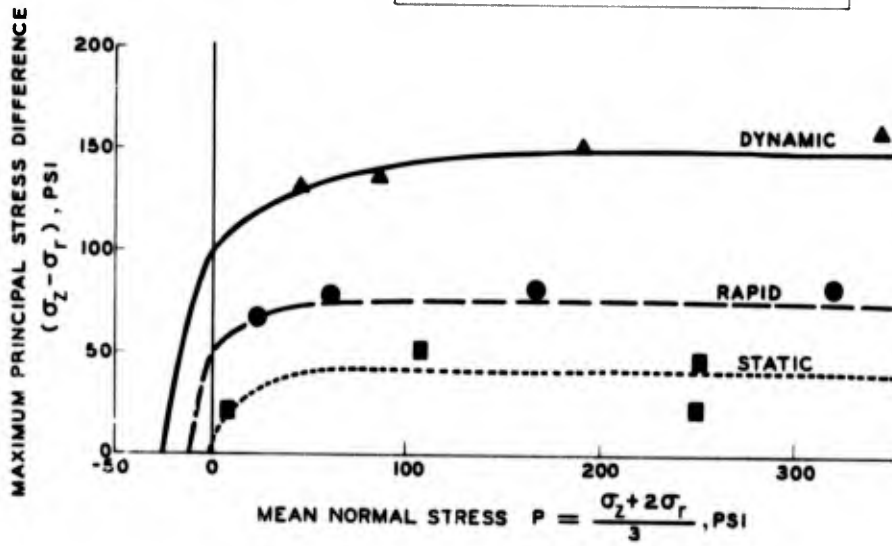


b. Dry site.

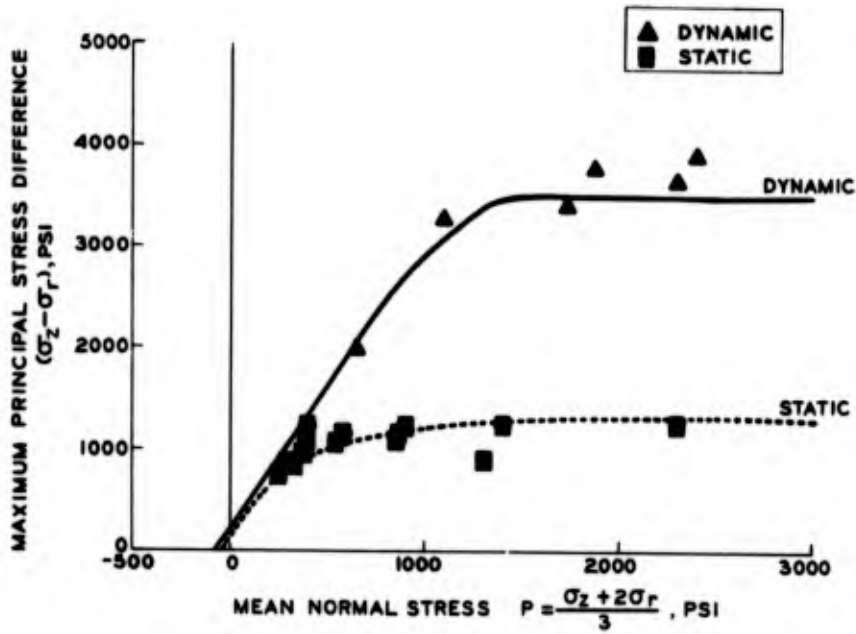
Figure 12. Comparison of representative initial constrained moduli with field seismic constrained moduli for MIDDLE GUST.

LOADING RATE FOR SHEAR PHASE OF TX TESTS

- ▲ DYNAMIC, < 50 MSEC TO FAILURE
- RAPID, 1 SEC TO FAILURE
- STATIC, 5 MINUTES TO FAILURE

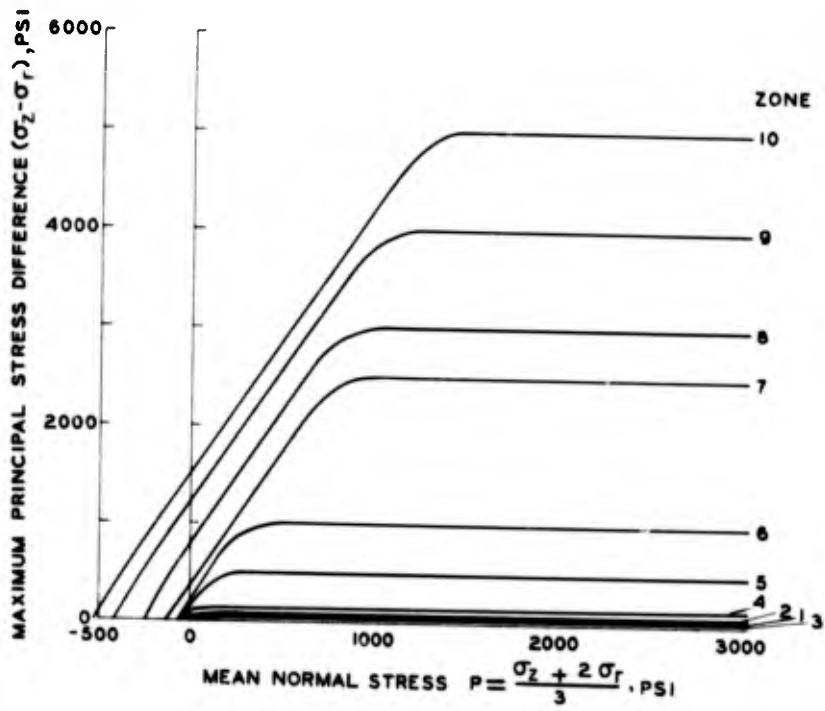


a. Zone 4, MIDDLE GUST wet site.

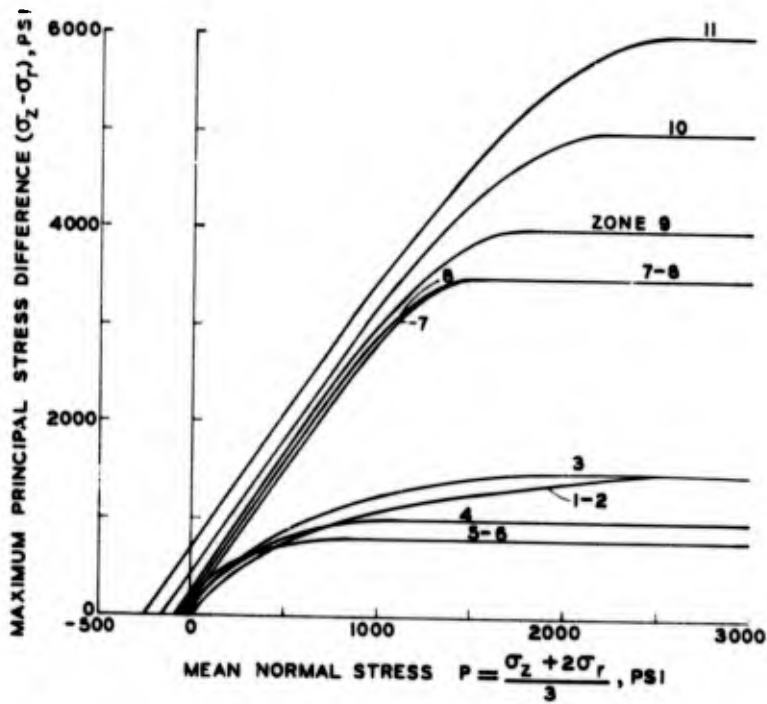


b. Zone 8, MIDDLE GUST dry site.

Figure 13. Representative preshot failure envelopes compared with typical TX data for selected zones.



a. Wet site.



b. Dry site.

Figure 14. Comparison of dynamic failure envelopes recommended preshot for MIDDLE CUST.

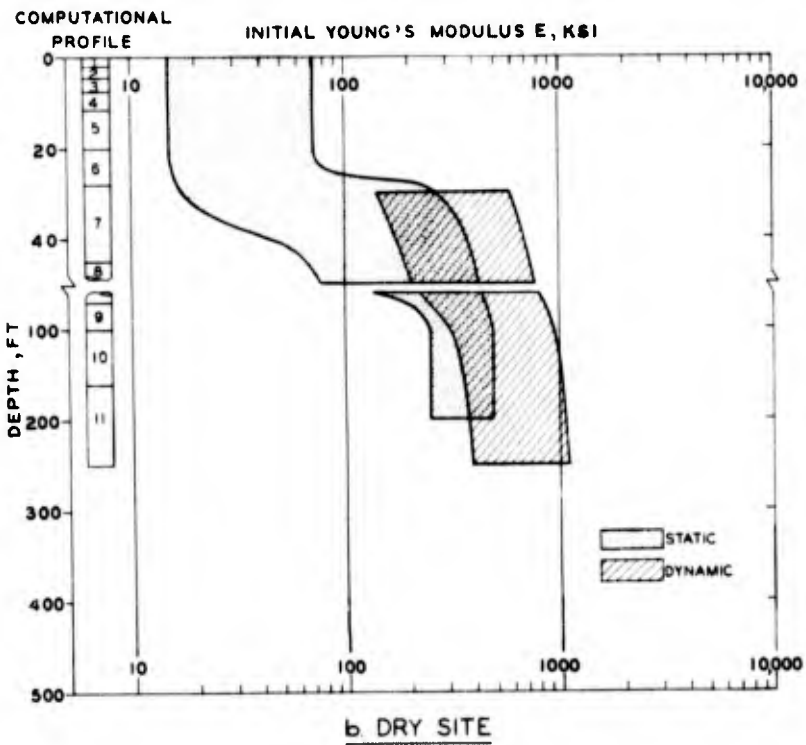
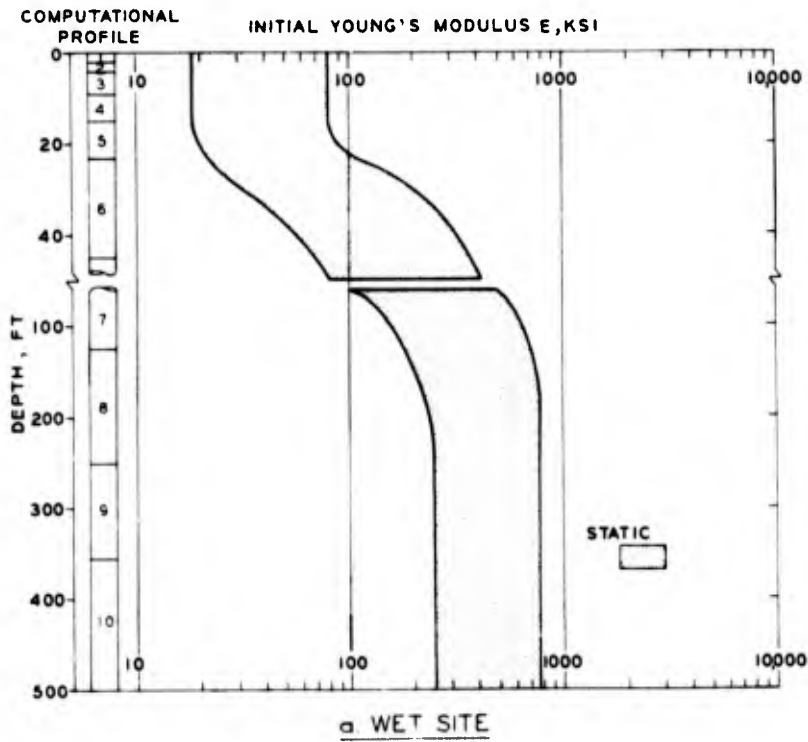


Figure 15. Comparison of initial Young's modulus data bands for MIDDLE GUST.

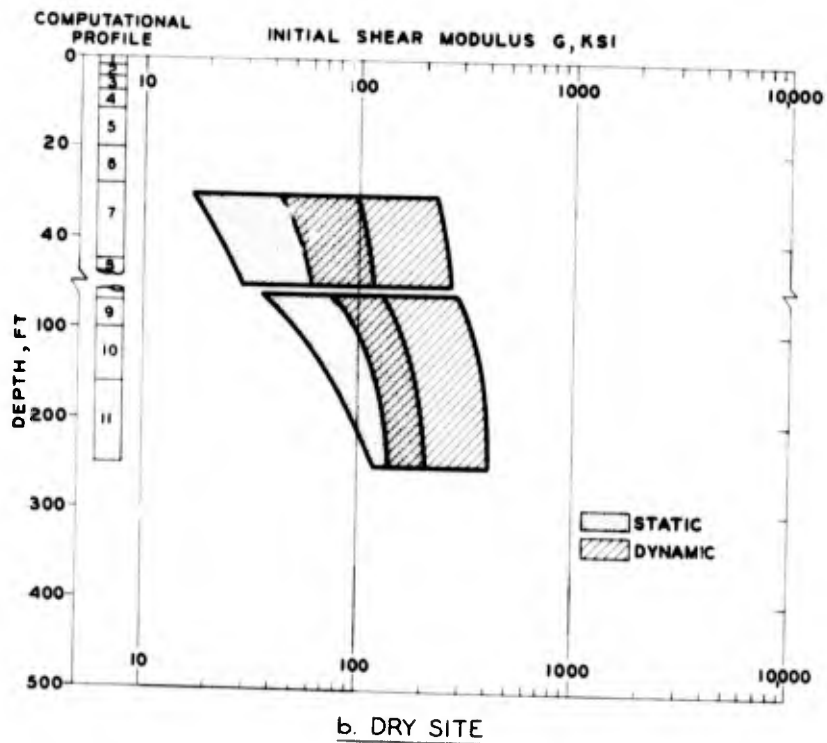
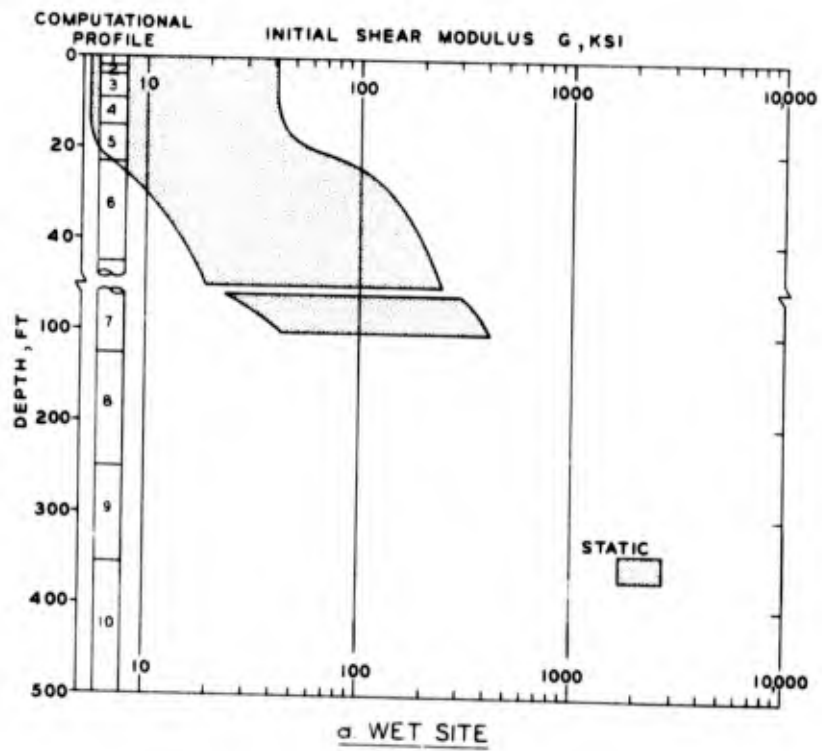
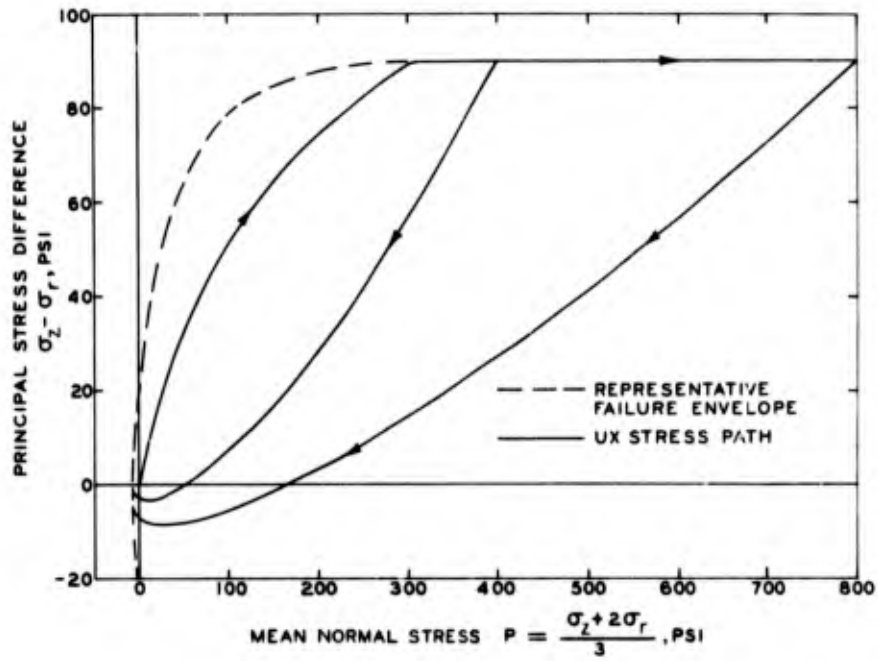
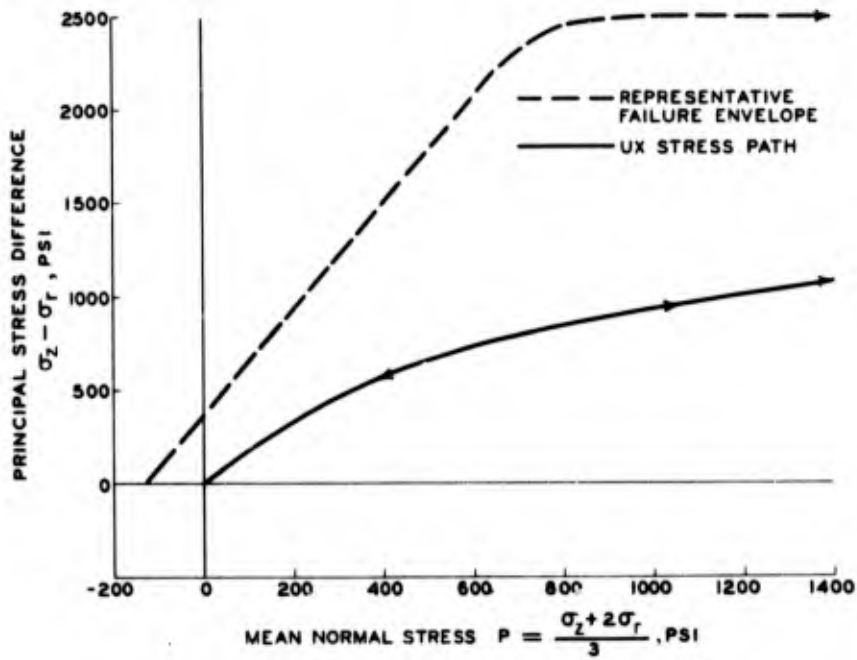


Figure 16. Comparison of initial shear modulus data bands for MIDDLE GUST.



a. ZONE 2, MIDDLE GUST WET SITE



b. ZONE 7, MIDDLE GUST WET SITE

Figure 17. Comparison of representative preshot uniaxial strain stress paths with failure envelopes for selected zones.

REFERENCES

1. J. E. Windham; U. S. Army Engineer Waterways Experiment Station, CE, Vicksburg, Miss.; Informal communication to: R. J. Port; Air Force Weapons Laboratory, Kirtland Air Force Base, N. Mex.; Subject: "Material Properties for Preshot Calculation of Middle Gust Event I"; July 1971; Unclassified.
2. J. P. Sale; U. S. Army Engineer Waterways Experiment Station, CE, Vicksburg, Miss.; Letter to: L. S. Melzer; Air Force Weapons Laboratory, Kirtland Air Force Base, N. Mex.; Subject: "Transmittal of Representative Material Properties for Preshot Calculations of Middle Gust Events II and III"; 30 September 1971; Unclassified.
3. J. S. Zelasko; U. S. Army Engineer Waterways Experiment Station, CE, Vicksburg, Miss.; Letter to: L. S. Melzer; Air Force Weapons Laboratory, Kirtland Air Force Base, N. Mex.; Subject: "Transmittal of Representative Material Properties for Preshot Calculations of Middle Gust Events IV and V"; 25 May 1972; Unclassified.
4. B. P. Bonner and others; "High Pressure Mechanical Properties of Shales and Regolith from the Middle Gust Site"; Report UCID-16104, September 1972; Lawrence Livermore Laboratory, University of California, Livermore, Calif.; Unclassified.
5. E. E. Jaramillo; "Data Report, Middle Gust I"; Report AL-831-1, July 1972; EG&G, Albuquerque Division, Government and Commercial Systems Group, Albuquerque, N. Mex.; Unclassified.
6. E. E. Jaramillo; "Data Report, Middle Gust V"; Report AL-831-5, April 1973; EG&G, Albuquerque Division, Government and Commercial Systems Group, Albuquerque, N. Mex.; Unclassified.
7. J. G. Jackson, Jr.; "Uniaxial Strain Testing of Soils for Blast-Oriented Problems"; Miscellaneous Paper S-68-17, September 1968; U. S. Army Engineer Waterways Experiment Station, CE, Vicksburg, Miss.; Unclassified.

In accordance with ER 70-2-3, paragraph 6c(1)(b), dated 15 February 1973, a facsimile catalog card in Library of Congress format is reproduced below.

Windham, Jon E

Geology and material property comparisons for the Middle Gust test sites, by J. E. Windham, R. A. Knott and J. S. Zelasko. Vicksburg, U. S. Army Engineer Waterways Experiment Station, 1974.

47 p. illus. 27 cm. (U. S. Waterways Experiment Station. Miscellaneous paper S-74-7)

Sponsored by Defense Nuclear Agency under Subtask SB209, Work Unit 11.

References: p. 35.

1. Geologic materials. 2. Laboratory tests. 3. Middle Gust (Series). 4. Constitutive properties. 5. Subsurface exploration. I. Knott, Randy A., joint author. II. Zelasko, Joseph S., joint author. III. Defense Nuclear Agency. (Series: U. S. Waterways Experiment Station, Vicksburg, Miss. Miscellaneous paper S-74-7)
TA7.W34m no.S-74-7